Methylene blue removal using a low-cost activated carbon adsorbent from tobacco stems: kinetic and equilibrium studies

Bellington Mudyawabikwa, Henry H. Mungondori, Lilian Tichagwa and David M. Katwire

ABSTRACT

The aim of this study was to prepare activated carbon from tobacco stalks using microwave heating. The prepared activated carbon was applied as an adsorbent in methylene blue (MB) removal from water. The optimum conditions for activated carbon preparation were a radiation power of 280 W for a period of 6 minutes after the impregnation of the precursor material with 30% $ZnCl_2$ for 24 hours. The activated carbon yield and iodine number were 49.43% and 1,264.51 mg/g respectively. The activated carbon also had a point of zero charge of 5.81 with an adsorption capacity of 123.45 mg/g for MB. The optimum conditions for MB adsorption were a pH of 6.5 with an adsorbent dosage of 0.2 g/50 mL at 25 °C. The MB adsorption kinetics followed the pseudo second order kinetic model with the intra-particle diffusion model suggesting a two-step adsorption mechanism. The adsorption data also fitted well within the Langmuir adsorption isotherm model. Tobacco stalks can successfully be turned into an economically important product.

Key words | activated carbon, adsorption isotherms, adsorption kinetic models, intra-particle diffusion model, methylene blue

Bellington Mudyawabikwa
Tobacco Research Board,
P.O. Box 1909 Airport Ring road,
Harare,
Zimbabwe

Henry H. Mungondori (corresponding author)
Lilian Tichagwa
David M. Katwire
Department of Chemistry,
University of Fort Hare,
1 King Williams Town Road,
Alice 5700,
Republic of South Africa
E-mail: *henrymungondori@gmail.com*

Lilian Tichagwa
Department of Polymer Technology and Engineering,
Harare Institute of Technology,
Ganges Road,
Belvedere,
Zimbabwe

INTRODUCTION

Synthetic dyes are one of the major water pollutants, with their presence in water even in low quantities highly visible and undesirable. The colour itself interferes with sunlight penetration and retards photosynthesis, thereby inhibiting the growth of plant biota (Wang *et al.* 2005). Direct discharge of dyes into the environment may also result in the formation of toxic carcinogenic breakdown products. The conventional methods for the treatment of wastewater containing dyes include chemical oxidation (Oguz & Keskinler 2007), liquid–liquid extraction (Muthuraman *et al.* 2008) and adsorption (Mohan *et al.* 2002). All these methods have certain limitations, which include low efficiency and limited scope. Adsorption has however been considered to be a better method because of its simplicity in design, operation and convenience. The extent of adsorption depends on the nature of adsorbent, especially its surface area and porosity, and in light of this, various adsorbents have been developed with different properties. Amongst the many adsorbents in use, activated carbon has been the most popular and widely used adsorbent (Bhatnagar & Minocha 2006). Methylene blue (MB) adsorption from aqueous solution has been successfully accomplished using activated carbon adsorbent prepared from different precursor materials, which include cotton stalk (Deng *et al.* 2009), pistachio shells (Attia *et al.* 2003) and *Lupinus albus* (Bağcı & Ceyhan 2015). The adsorption capacities found were high in some cases, such as 193.5 mg/g for cotton stalks.

Activated carbon is produced by a process which involves dehydration, carbonization and activation of the raw materials. Some of the most popular activating agents for the chemical process are zinc chloride (Makeswari & Santhi 2012), H_3PO_4 (Zhong *et al.* 2012), K_2CO_3 (Li *et al.* 2008) and H_2SO_4. Other chemicals, which include Na_2CO_3, NaOH, $Ca(OH)_2$ and the chloride salts of magnesium, calcium, ferric iron and aluminium, have been used. The common feature in all these chemicals is their dehydrating nature. However, these different activating agents are affected by different parameters.

doi: 10.2166/wst.2017.041

Some countries producing substantial quantities of tobacco have challenges concerning the disposal of remaining stalks after reaping the leaves. Clearly, this represents a huge and untapped resource since these stems are considered as waste and unusable. Tobacco stems have been applied in the form of tobacco dust (Qi & Aldrich 2008), tobacco stem ash (Ghosh & Reddy 2013) and plain tobacco stems (Li *et al.* 2008) for the adsorption of metals and organic impurities in water. Activated carbon has been prepared from tobacco stems using potassium carbonate and phosphoric acid as activation agents (Li *et al.* 2008). Microwave assisted activated carbon preparation with zinc chloride activation from tobacco stalks has not been studied before the current study. The performance of the activated carbon prepared from tobacco stalks in the adsorption of MB has also not been studied. The focus of this study was therefore to prepare activated carbon from tobacco stalks using $ZnCl_2$ as an activating agent and to apply the activated carbon as an adsorbent for the removal of MB from aqueous solutions.

MATERIALS AND METHODS

Materials and equipment

The tobacco stems were obtained from Mashonaland east province of Zimbabwe. The following chemicals were used: zinc chloride ($ZnCl_2$) (98% Merck, Germany), hydrochloric acid (HCl) (37% Merck, Germany), nitric acid (HNO_3) (65% Merck, Germany), sodium nitrate ($NaNO_3$) (99% Sigma-Aldrich, Germany), and sodium hydroxide (NaOH) (97% Sigma-Aldrich, Germany).

The following equipment was used in the experiments: grinder with sieve, Sartorius analytical balance, Hisense microwave oven MM717AOH model with output of up to 700 W, domnick hunter nitrogen generator, oven, Innova 4000 incubator shaker, UV-Vis spectrometer (Perkin Elmer lambda 25), flame atomic absorption spectrometer (FAAS) (Perkin Elmer 900F), Shimadzu Fourier transform infrared spectrometer (FTIR), PanAlytical X'pert Pro PW3040/60 X-ray diffractometer, automatic chemisorption and physisorption analyser, Tristar II 3020 V1.02, Eutech pH and conductivity meter.

Preparation of adsorbent

The fresh tobacco stems were washed with water, air dried for 72 hours, ground and sieved through a 1 mm sieve. A 6 g sample of the powdered and dried raw material was mixed with 30 mL $ZnCl_2$ of concentration in the range of 30 to 60% w/v. The slurry was kept at room temperature for 18 to 26 hours to ensure thorough mixing of the $ZnCl_2$ with tobacco stems. After the impregnation period, the slurry in a ceramic crucible was placed in a microwave heating apparatus connected to a nitrogen generator producing a continuous stream of nitrogen. Carbonization was done for 4 to 10 minutes at a microwave power in the range 140 to 560 W. The carbonized samples were washed with 0.1 M HCl, hot water and then distilled water until the pH of the washing solution reached 6–7. The material was then dried at 110 °C overnight and finally powdered using a pestle and mortar.

Table 1 | Design factors and levels

	Range and values				
Independent variable	**Symbol**	**1**	**2**	**3**	**4**
Radiation power (W)	A	140	280	420	560
Radiation time (minutes)	B	4	6	8	10
Concentration of $ZnCl_2$ (Vol. %)	C	30	40	50	60
Impregnation time (hours)	D	18	22	24	26

The Taguchi experimental design was used to optimize the preparation conditions. The four operational variables are shown in Table 1.

From the four operational parameters, an L_{16} orthogonal array was used to evaluate the optimal values as shown in Table 2.

Yield and iodine number

The activated carbon yield from the air-dried tobacco stems, Y, was calculated using the equation:

$$Y = \frac{M}{M_0} \times 100 \quad (1)$$

where M is the weight of activated carbon and M_0 is the weight of air-dried tobacco stems.

Iodine number was determined using the (ASTM 2006) International standard test method for the determination of iodine number of activated carbon. The preparation conditions which gave the optimum yield and iodine number were selected for further studies.

Table 2 | Experimental design matrix

	Variables			
Sample ID	**A**	**B**	**C**	**D**
TS 1	1	1	1	1
TS 2	2	1	1	1
TS 3	3	1	1	1
TS 4	4	1	1	1
TS 5	1	1	1	1
TS 6	1	2	1	1
TS 7	1	3	1	1
TS 8	1	4	1	1
TS 9	1	1	1	1
TS 10	1	1	2	1
TS 11	1	1	3	1
TS 12	1	1	4	1
TS 13	1	1	1	1
TS 14	1	1	1	2
TS 15	1	1	1	3
TS 16	1	1	1	4

Adsorption studies

Adsorption studies were carried out using different adsorbent dosages (0.1 g–1.0 g), pH (2–10), initial analyte concentration (50–600 mg/L) and adsorption time (10–120 min) in accordance with (Namasivayam & Sangeetha 2005) study. Adsorption was carried out in an incubator shaker at 180 rpm and 25 °C. After the shaking period, the solution was filtered through a Whatman (number 541) filter paper. MB was analysed on a UV/Vis spectrometer at a wavelength of 664 nm. The amount adsorbed on the activated carbon was calculated using the mass balance relationship represented by Equation (2):

$$q_t = \frac{(C_0 - C_t)V}{W}, \quad (2)$$

where q_t is the amount of MB adsorbed at time t, C_0 is the initial MB concentration in solution and C_t is the final (at time t) liquid phase concentration of MB. V is the volume of solution in litres and W is the adsorbent weight in grams.

The removal percentage was calculated using the equation:

$$\text{Removal } \% = \frac{C_0 - C_t}{C_0} \times 100, \quad (3)$$

where C_0 and C_t are the initial and final (at time t) liquid phase concentrations of analyte, respectively.

Adsorption kinetics studies

Adsorption kinetics studies were carried out at 25 °C using three concentrations of 100 mg/L, 150 mg/L and 200 mg/L. Adsorption time was set at 100 minutes with pH of solution at 6.5 and an adsorbent dosage of 0.2 g/50 mL.

Adsorption isotherm studies

Adsorption isotherm studies were carried out at 25 °C with the optimum conditions used in the kinetics studies maintained.

Characterization

Physical characterization as well as chemical characterization was done on the activated carbon product.

Zero surface charge (pH_{zpc})

The pH_{zpc} was determined using the solid addition method in a series of 250 mL glass stoppered flasks. Each flask was filled with 50 mL of 0.1 M $NaNO_3$ solution at different initial pH and 0.2 g of activated carbon. The pH values were adjusted between 2 and 10 using 0.1 M HNO_3 or 0.1 M NaOH. The suspensions were tightly closed and shaken at 150 rpm for 2 hours. The final pH of the supernatant was determined and the pH_{zpc} was determined by plotting (pH_i – pH_f) against pH_i, where pH_i and pH_f were the initial and final pH values of the solution, respectively. The pH_{zpc} is the point of intersection of the resulting curve with the abscissa where (pH_i – pH_f) = 0.

Conductivity, carbon content, ash content and specific gravity

Conductivity was measured in 50 mL double distilled water using a conductivity meter. The specific gravity was determined using a pycnometer, while the ash content was determined through combusting the activated carbon in an oxidizing muffle furnace. The ash was also analysed for sodium, potassium, calcium, iron and zinc using an FAAS. The carbon content was determined using the ashing method at 550 °C in a muffle furnace.

Fourier transform infrared spectroscopy

A Shimadzu FTIR with KBr pellet was used to study the surface functional groups of the activated carbon in the scanning range of 4,000–400 cm^{-1}.

Porosity

The surface porosity of the activated carbon was characterized using an automatic chemisorption and physisorption analyser with N_2 being the adsorbate at 77.3 K. The specific surface area and total pore volume were calculated from the Brunauer–Emmett–Teller (BET) equation, whereas the microporosity and mesoporosity were determined using the v-t and the Barrett–Joyner–Halenda (BJH) methods respectively.

X-ray diffraction spectroscopy

X-ray powder diffraction (XRD) pattern of the activated carbon was obtained on an X'pert PRO diffractometer from PanAlytical with Ni filtered Cu K-α of wavelength 0.1542 nm with radiation at 35 KV and 40 mA.

RESULTS AND DISCUSSION

Yield and iodine number

The effect of different variables on the preparation of activated carbon was determined using the L_{16} array in accordance with the Taguchi method. Sixteen different activated carbon samples were prepared and the iodine number and yield of each were determined with the results shown in Table 3. The yield and iodine number results are graphically represented in Figure 1.

Figure 1 shows the effect of each operational parameter on the yield and iodine number of the prepared activated carbon. The effects of radiation power were evaluated under a $ZnCl_2$ concentration of 30% for 4 minutes. Figure 1(a) shows that the yield increased when radiation power was increased from 140 W to 280 W. Increasing radiation power from 280 W to 560 W had no major impact on activated carbon yield. The same trend was also observed with adsorption capacity as depicted by the iodine number. The possible reason for increase in yield and adsorption capacity with increasing microwave power could be that the higher energy on the samples resulted in more active sites and pores being created in the final product. Similar results were also obtained by other researchers (Makeswari & Santhi 2012).

Table 3 | Optimization results

Sample ID	Iodine number	Yield
TS 1	725.60	39.79
TS 2	902.63	46.70
TS 3	913.45	46.68
TS 4	906.77	46.91
TS 5	736.12	41.25
TS 6	1,281.52	49.45
TS 7	1,212.67	48.34
TS 8	1,197.56	48.33
TS 9	781.34	39.26
TS 10	801.32	39.33
TS 11	789.00	38.96
TS 12	760.31	39.32
TS 13	782.45	44.61
TS 14	791.45	44.89
TS 15	788.14	44.96
TS 16	790.54	44.94

The effects of radiation time were evaluated under $ZnCl_2$ concentration of 30% and radiation power of 100 W. Figure 1(b) shows that both the yield and iodine number increased when radiation time was increased from 4 minutes to 6 minutes. A further increase in radiation time, however, resulted in a slight decrease in both the yield and iodine number. The possible explanation for this could be that the prolongation of radiation time from 4 minutes to 6 minutes resulted in the formation of more active sites and pores on the activated carbon surface. A further increase in radiation time, however, might have resulted in the burning off of the carbon pores by microwave heat, resulting in lower yield and iodine number. This observation was also reported by other researchers (Li *et al.* 2008). Figure 1(c) and 1(d) show that increasing $ZnCl_2$ concentration and impregnation time had no major impact on the yield and iodine number. The results, however, show that optimum parameters could be obtained at a $ZnCl_2$ concentration of 30% for an impregnation time of 24 hours. Table 4 shows a comparison of the yield and iodine number obtained from the activated carbon produced from tobacco stems in this current study with some studies reported in the literature. The activated carbon yield obtained with tobacco stems is better than with most of the agricultural waste products due to the high carbon

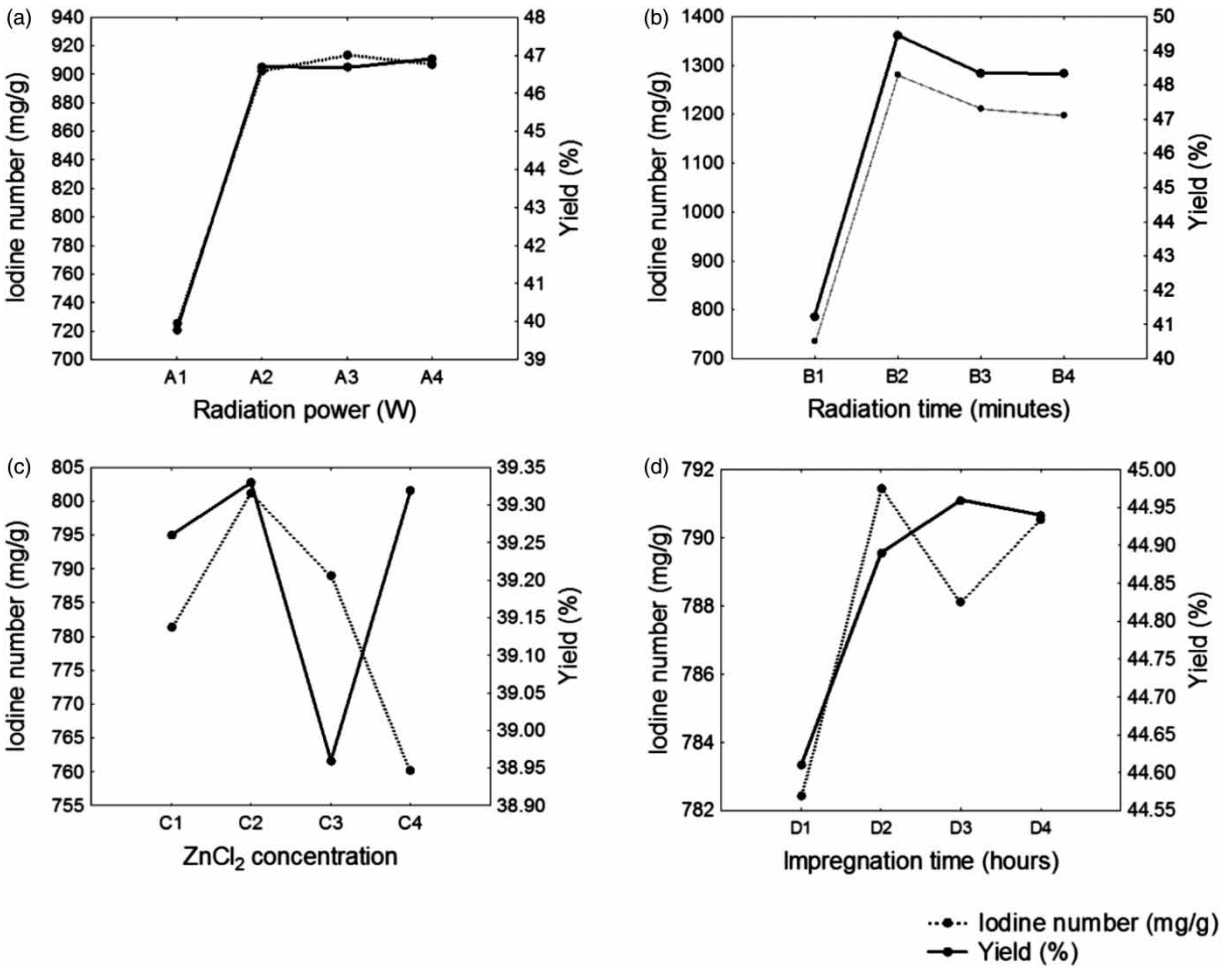

Figure 1 | Operational parameters' effects on the responses of activated carbon prepared from tobacco stalks: (a) radiation power, (b) radiation time, (c) $ZnCl_2$ concentration and (d) impregnation time.

content of the precursor material. The iodine number is also better than for the activated carbon produced from the other precursor materials except for *Ricinus communis*.

Table 4 | Yield and iodine number of activated carbon from different precursor materials

Precursor	Agent	Yield (%)	Iodine number (mg/g)	Reference
Peanut hull	H_3PO_4	42.12	813.11	Zhong *et al.* (2012)
Coconut coir pith	$ZnCl_2$		203.00	Namasivayam & Sangeetha (2005)
Bagasse	H_3PO_4	53.60	626.00	Lori *et al.* (2008)
Ricinus communis	$ZnCl_2$	58.18	1,797.93	Makeswari & Santhi (2012)
Sorghum	H_3PO_4	30.60	667.00	Lori *et al.* (2008)
Millet straws	H_3PO_4	29.60	593.00	Lori *et al.* (2008)
Tobacco stem	$ZnCl_2$	49.43	1,264.51	Current study

Optimum conditions

The product yield and adsorption capacity were the major attributes of interest that needed to be optimized. Radiation power and time had major effects on product yield and adsorption capacity, with impregnation time and $ZnCl_2$ concentration having little contribution. The adopted optimal conditions are presented in Table 5.

The activated carbon produced using the optimum conditions was further characterized and used in adsorption experiments.

Point of zero charge (pH_{pzc})

An adsorbent's point of zero charge is an important characteristic, which determines the point at which the adsorbent surface has net electrical neutrality. Figure 2 shows a plot of

Table 5 | Optimized conditions for the preparation of activated carbon from tobacco stalks

	Parameter				Results	
	Radiation power (W)	Radiation time (minutes)	Impregnation time (hours)	$ZnCl_2$ concentration (%)	Yield (%)	Iodine number (mg/g)
Level	280	6	24	30	49.43	1,264.51

(pH_i – pH_f) versus pH_i. The point of zero charge obtained from the plot is 5.81, indicating that the pH_{pzc} is less than the solution pH at 7.00, causing an increase in the negative charge density on the surface of activated carbon, which should foster the adsorption of cations.

The activated carbon prepared using optimum conditions was analysed for its physical and chemical characteristics. Table 6 shows the physical and chemical characteristics of the activated carbon prepared from tobacco stalks.

FTIR analysis

The functional groups on the surface of the activated carbon contribute significantly to the adsorption ability of the activated carbon as adsorbents, catalysts, catalyst supports and ion exchangers (Ren *et al.* 2011). The FTIR spectrum in Figure 3 revealed that the prepared activated carbon contains fewer bands than the tobacco stems. The broad band at 3,299.66 cm^{-1} in the spectrum for tobacco stems was assigned to the O-H stretching vibrations of the hydroxyl groups which included hydrogen bonding. This band is less intense in the spectrum of the prepared activated carbon, which is a sign of cellulosic and lignocellulosic material degradation. The peak around 2,900 cm^{-1} for both the activated carbon and precursor material is indicative of aliphatic groups (-CH_2-) in both materials, although it is less intense in the activated carbon, while those appearing around 1,592 cm^{-1} in the precursor and 1,496 cm^{-1} in the activated carbon spectra can be attributed to the –C=C– aromatic ring stretch. Significant differences in the spectra were noted in the bands between 1,740 and 1,000 cm^{-1}. The precursor material had a peak at 1,743 cm^{-1}, which was ascribed to C=O, and another one at 1,224 cm^{-1}, which may be attributed to esters, ethers or polyphenol groups. These peaks are no longer present in the activated carbon spectrum, showing the elimination of hydrogen and oxygen during activated carbon formation. The peak appearing at 1,029 cm^{-1} in the precursor can be attributed to primary C–O stretch. This has been greatly weakened in the activated carbon, further giving evidence of oxygen and hydrogen elimination.

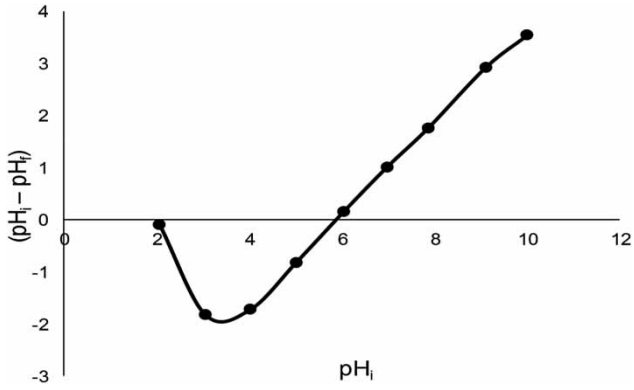

Figure 2 | Zero point charges of activated carbon prepared from tobacco stalks.

BET surface area analysis

Figure 4 shows a plot of the BET N_2 adsorption isotherms at 77.3 K for the activated carbon. The isotherm shape can be

Table 6 | Physical and chemical properties of prepared activated carbon

Physical/Chemical parameter	Result
pH_{zpc}	5.81
Conductivity (1% solution)	131 µS/cm
Ash	0.16%
Specific gravity	0.54 g/cm^3
Carbon content	99.84%
Iodine number	1,264.51
Zinc	0.01%
Ash analysis	
Na	<0.01%
K	6.33%
Ca	<0.01%
Mg	<0.01%
Fe	<0.01%
Mn	<0.01%
Cu	0.92%

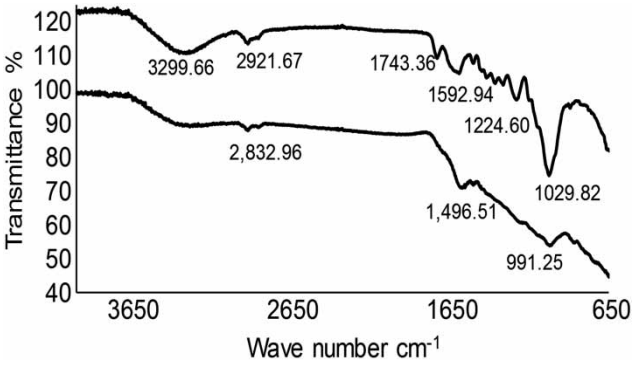

Figure 3 | FTIR spectra of tobacco stems (a) and tobacco stems based activated carbon (b).

classified as a type 1 character according to the International Union of Pure and Applied Chemistry classification. This is an indication that the activated carbon is more microporous than mesoporous.

Table 7 shows the BET parameters of the activated carbon with a BET surface area of 684.68 m^2/g and a pore volume of 0.45 cm^3/g, which are quite comparable to activated carbon obtained from other precursor materials (Tamilselvi & Asaithambi 2015).

Pore size distribution

The micropore size analysis was done using the (v-t) method. Table 8 shows the micropore parameters.

The activated carbon has a micropore volume of 0.03 cm^3/g and area of 233.17 m^2/g. The material would therefore be most suitable as a liquid adsorbent due to the low micropore volume.

The mesopore size distribution analysis was done using the BJH method. The desorption isotherm of the BJH

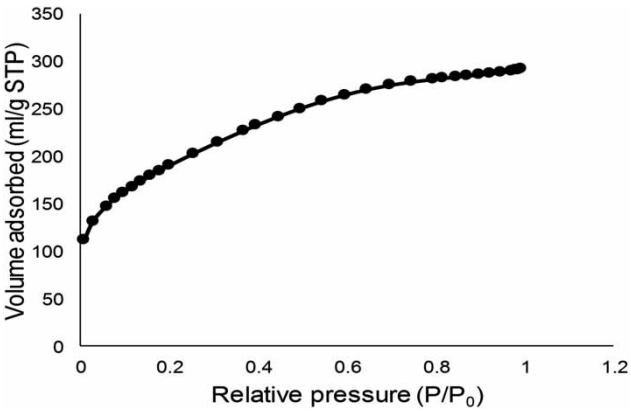

Figure 4 | N_2 adsorption isotherm at 77.3 K of tobacco stalks based activated carbon.

Table 7 | N_2 BET parameters

Parameter	Value
BET linear equation	$y = 0.006305x + 0.000053$
S_{BET} (m^2/g)	684.68
BET constant (C)	119.13
R^2	0.99
Pore volume (cm^3/g)	0.45

method was used. Figure 5 shows a plot of incremental pore volume versus pore width in the mesopore region. The distribution curve suggests a predominant mesopore due to the sharp increase between a pore width of 2 nm and 5 nm. The average pore diameter of the activated carbon is 3.30 nm.

XRD analysis

The XRD pattern of the activated carbon is shown in Figure 6. The broad peak appearing between 25° and 27° shows the presence of carbon.

There are no other peaks showing on the XRD, meaning that there are no other X-ray traceable compounds in the activated carbon sample. This confirms the removal of the $ZnCl_2$ employed as the activating agent.

Effect of adsorption time on MB adsorption

Figure 7 illustrates the effect of adsorption time on the removal of MB from aqueous solution. The experiment was conducted at 25 °C using an adsorbent dosage of 0.1 g at a pH of 6.5. The MB concentration that was used in this study was 150 mg/L.

MB adsorption increased with an increase in contact time. The rate of removal was rapid in the first 40 minutes and then it tended to level thereafter, proceeding at a slower rate until saturation was obtained. This suggests a rapid adsorption on the external surface of the adsorbent,

Table 8 | Activated carbon micropore parameters

Parameter	Value
Micropore volume (cm^3/g)	0.03
Micropore area (m^2/g)	233.17
External surface area (m^2/g)	451.51
Total surface area (m^2/g)	684.68

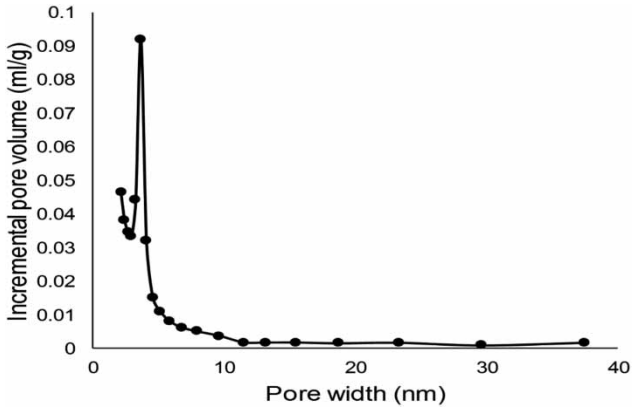

Figure 5 | Mesopore size distribution by the BJH method.

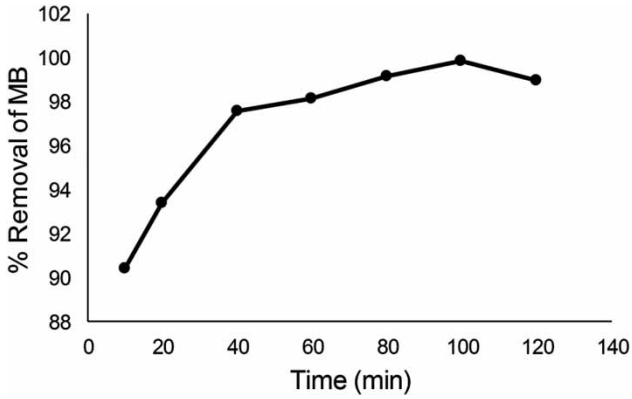

Figure 7 | Effect of adsorption time on MB removal: adsorbent dose, 0.1 g/50 mL; pH 6.5; MB concentration, 150 mg/L and temperature, 25 °C.

which was then followed by a rate determining step of an internal diffusion process. At the inception of the adsorption process, the vacant active sites on the surface of the activated carbon fill up quickly, and a decrease in the available active sites resulted in the attenuation of the diffusion rate. This observation was also reported in literature (Bağcı & Ceyhan 2015). The observed optimum time for MB removal was 100 minutes. There was a slight decrease in MB removal after 100 minutes, which might have been due to an increased collision between the particles of the adsorbate and adsorbent, which weakened the interaction between the two, thus releasing the MB into solution. This observation was also noted by Said *et al.* (2014).

Effect of initial concentration of MB

In this study, the effects of MB concentration on percentage removal were investigated using initial MB concentrations of 50 mg/L, 100 mg/L, 150 mg/L, 200 mg/L, 300 mg/L, 500 mg/L and 600 mg/L. Figure 8 shows the variation of percentage removal of MB from aqueous solution with different initial concentrations.

Adsorption tends to be higher at high concentration when equilibrium has been attained. This is due to the fact that the vacant active sites on the adsorbent tend to fill up quickly at higher initial concentrations because mass transfer resistance between solid surface and solution is easily overcome. Percentage rate of removal is, however, inversely proportional to the increasing initial concentration because the ratio of MB concentration in solution to the number of active sites on the adsorbent is lower. This also implies that competition of MB molecules for adsorption to the surface is low at low initial concentrations.

Effect of adsorbent mass

Experimental studies to determine the effects of dosage of adsorbent on adsorption were carried out using MB of initial

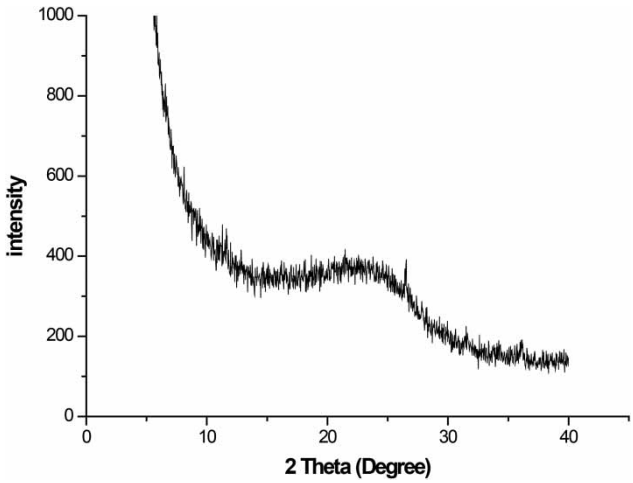

Figure 6 | XRD pattern of the activated carbon from tobacco stalks.

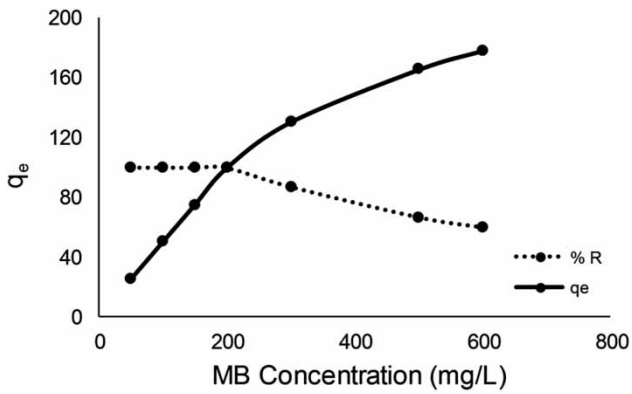

Figure 8 | Effect of MB initial concentration: adsorbent dosage, 0.1 g/50 mL; pH, 6.5; adsorption time, 120 minutes and temperature, 25 °C.

concentration of 150 mg/L at a pH of 6.5 for 120 minutes. The results of the effects are shown in Figure 9. MB adsorption increased rapidly up to an adsorbent dosage of 0.2 g, a stage at which there was a gradual increase in adsorption. This trend can be explained by an increase in the volume of active sites with increasing dosage. However, increasing the volume of active sites after equilibrium has been observed to have no effect on the adsorption capacity. The adsorbent mass that was adopted for further experiments in this study was 0.2 g.

Effect of pH

The effect of pH on percentage removal of MB was assessed within the pH range of 2 to 10 using MB initial concentration of 150 mg/L at 25 °C for 120 minutes. Figure 10 shows the relationship between pH and MB uptake.

MB uptake increased when pH was increased from 2 to 5, after which the rate of adsorption levelled up to pH 7. This was probably because the point of zero charge of the activated carbon was 5.81, and at pH values less than this, the surface charge of the activated carbon tends to be positive, making the hydronium ions in solution effectively compete with the cationic MB, an observation that was also reported in literature (Amuda *et al.* 2014). After pH 7, the percentage removal of MB started to decline as the pH was increased. This result agrees with the findings of other researchers (Gercel *et al.* 2007). Tahiruddin & Ab Rahman (2013) obtained similar results and proposed that this might have been due to the hydroxide ions reacting with the cationic analyte at high pH and as a result decreasing the adsorption of the analyte. The solution pH adopted for further experiments was 6.5.

MB adsorption kinetics

The kinetic study of adsorption is important, since it is a depiction of adsorbate uptake rate and also a controlling parameter to the adsorption process residual time. The experimental data in this study were fitted to the pseudo first order, pseudo second order and intra-particle diffusion models.

The rate equation for the pseudo first order kinetic model is expressed as:

$$\frac{dq_t}{dt} = K_1(q_e - q_t) \tag{4}$$

where q_t and q_e are the adsorbate amounts (mg/g) adsorbed at time (t) and equilibrium, respectively, with K_1 being the pseudo first order rate constant.

On integration, it will give the linear form:

$$\ln(q_e - q_t) = \ln q_e - Kt, \tag{5}$$

of which a plot of ln $(q_e - q_t)$ versus t results in a linear graph confirming pseudo first order adsorption.

The pseudo second order equation is expressed as:

$$\frac{dq_t}{dt} = K_2(q_e - q_t)^2 \tag{6}$$

Separating the variables and integrating will result in the linear form of this model, which is:

$$\frac{t}{q_t} = \frac{1}{K_2 q_e^2} + \frac{t}{q_e} \tag{7}$$

A plot of (t/q_t) versus t would give a linear plot if the adsorption process followed the pseudo second order model.

Tables 9 and 10 list the kinetic model parameters and correlation coefficients for the different initial

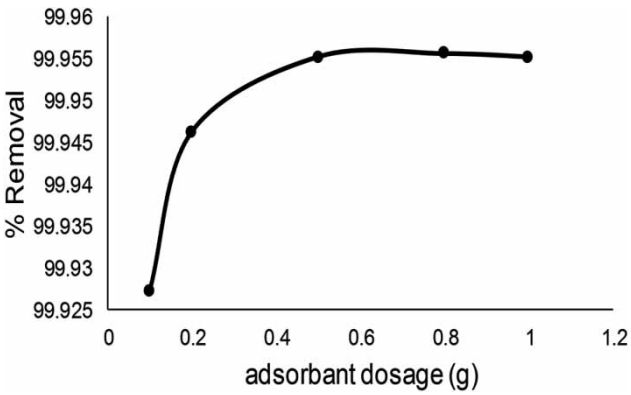

Figure 9 | Effect of adsorbent dosage on MB removal: initial concentration, 150 mg/L; pH, 6.5; adsorption time, 120 minutes and temperature, 25 °C.

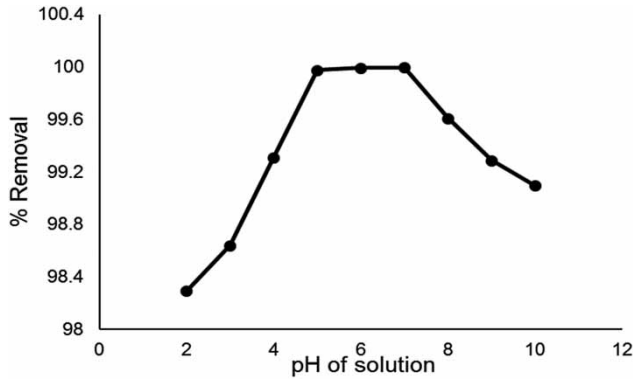

Figure 10 | Effect of pH on MB removal: Initial concentration, 150 mg/L; adsorbent dosage, 0.2 g/50 mL; adsorption time, 120 minutes and temperature, 25 °C.

Table 9 | Pseudo first order kinetic model parameters for MB adsorption

C_0 (mg/L)	$q_{e,exp}$ (mg/g)	Kinetic equation	k_1 (min^{-1})	$q_{e,cal}$ (mg/g)	R^2
100	49.95	$y = -0.0472x - 0.8441$	0.05	0.43	0.86
150	74.89	$y = -0.0363x + 2.2529$	0.04	9.52	0.98
200	99.60	$y = -0.0289x + 3.3124$	0.03	27.45	0.96

concentrations for the pseudo first order kinetic model and the pseudo second order, respectively.

It is apparent that the R^2 values obtained from the pseudo first order model are consistently lower than those from the pseudo second order model. The adsorption capacities (q_e) for the second order also coincide with the expected (q_e) values, whereas the calculated (q_e) values from the first order have a huge variance with the ($q_{e,exp}$). This indicates that the adsorption perfectly obeys the pseudo second order model.

Intra-particle diffusion

The intra-particle diffusion model evaluated in this study obeys Equation (8):

$$q_t = K_p t^{0.5} + C \tag{8}$$

where q_t is the adsorbate amount (mg/g) adsorbed at time (t), K_p is the intra-particle diffusion rate constant (mg/(g $t^{0.5}$)) and C is the intercept. The graph of q_t versus $t^{0.5}$ would yield a straight line passing through the origin when intra-particle diffusion is the only rate limiting step. The correlation coefficient (R^2) indicates the fitness of this model and the slope gives the value of the intra-particle diffusion coefficient. From the intra-particle diffusion parameters in Table 11, it is evident that the intercepts (C) at all the three concentrations were not passing through the origin, suggesting that other processes were affecting the adsorption process. The correlation coefficients are, however, relatively high, indicating that the intra-particle diffusion takes place alongside other processes which were also affecting adsorption.

Table 11 | Intra-particle diffusion model parameters for MB adsorption

C_0 (mg/L)	k_p (mg/(g $t^{0.5}$))	C	R^2
100	0.02	49.77	0.87
150	1.01	65.45	0.92
200	3.05	70.89	0.88

Adsorption isotherms

The equilibrium data in this experiment were analysed by fitting it into two isotherm models at 25 °C. The isotherm models used are the Langmuir and the Freundlich isotherm models.

Langmuir isotherm

The Langmuir model can be expressed linearly as:

$$\frac{C_e}{Q_e} = \frac{1}{Q_m} C_e + \frac{1}{bQ_m} \tag{9}$$

where C_e is the equilibrium concentration of analyte in liquid, Q_e is the equilibrium concentration of analyte in solid phase, Q_m is the Langmuir constant for maximum analyte uptake, b is the Langmuir sorption equilibrium constant.

The Langmuir isotherm model parameters obtained from the plot of(C_e/Q_e) versus C_e are indicated in Table 12.

Figure 11 further illustrates the Langmuir dimensionless constant factor R_L, which gives an indication of how favourable or unfavourable the isotherm is. The R^2 value for the Langmuir isotherm is one with the R_L values all between 0 and 1. This is an indication that the adsorption process fits the Langmuir isotherm well at the studied temperature.

Table 10 | Pseudo second order kinetic model parameters for MB adsorption

C_0 (mg/l)	$q_{e,exp}$ (mg/g)	Kinetic equation	k_1 (min^{-1})	$q_{e,cal}$ (mg/g)	R^2
100	49.95	$y = 0.02x + 0.0017$	0.235	50.00	1.00
150	74.89	$y = 0.0132x + 0.019$	0.009	75.76	1.00
200	99.60	$y = 0.0098x + 0.0357$	0.003	102.04	0.99

Table 12 | Isotherm model parameters and correlation coefficients for MB adsorption on activated carbon at 25 °C

	Langmuir isotherm model			Freundlich isotherm model		
Temperature (°C)	Q_m (mg/g)	b (L/mg)	R^2	K_f ((mg/g).(L/mg)$^{1/n}$	1/n	R^2
25	123.46	2.89	1.00	124.05	0.44	0.99

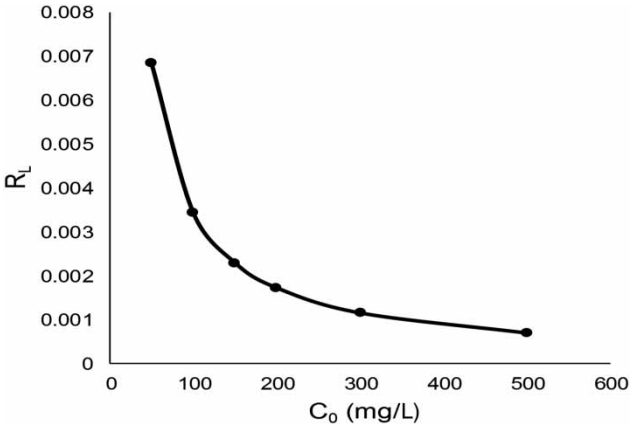

Figure 11 | R_L values under different initial concentrations of MB.

Freundlich isotherm

The Freundlich isotherm model can be expressed as:

$$Q_e = K_f C_e^{1/n}, \quad (10)$$

where Q_e and C_e are equilibrium concentrations of analyte in adsorbed and liquid phase respectively, K_f is the Freundlich constant indicating capacity, and n is the Freundlich constant indicating adsorption intensity.

Table 12 indicates the Freundlich parameter values as obtained from the plot of log Q_e versus log C_e.

Since the 1/n value is less than 1, it indicates favourability of adsorption. The R^2 value, however, is low, indicating that the equilibrium adsorption data do not fit well into the Freundlich model. The adsorption capacity of the adsorbent is also comparable to that obtained with the Langmuir model.

Adsorption thermodynamics

The Gibbs free energy change was calculated from the equation:

$$\Delta G^0 = -RT \ln (K_l), \quad (11)$$

where R is the universal gas constant (8.314 J/mol K), T is the temperature in Kelvins, and K_l is the equilibrium constant at the specific temperature.

The entropy change (ΔS^0) and the enthalpy change (ΔH^0) of the adsorption process were evaluated from the following equation:

$$\ln (K_l) = \frac{\Delta S^0}{R} - \frac{\Delta H^0}{RT}, \quad (12)$$

Table 13 | Thermodynamic parameters

Temp (K)	E_a (kJmol^{-1})	ΔG^0 (kJmol^{-1})	ΔH^0 (kJmol^{-1})	ΔS^0 (JK^{-1}mol^{-1})
298.15	44.20	−11.94	11.21	77.69
308.15		−12.75		
323.15		−13.88		

with the thermodynamic parameters being evaluated from the plot of $\ln K_l$ versus $(1/T)$.

The Arrhenius equation was used to evaluate the activation energy (E_a):

$$\ln (K_1) = \ln A - \frac{E_a}{RT}, \quad (13)$$

with K_2 being the equilibrium rate constant for the pseudo second order adsorption and A the pre-exponential factor. E_a was evaluated from the plot of $\ln K_1$ versus $(1/T)$.

The adsorption thermodynamic parameters are shown in Table 13. The negative values for ΔG^0 indicate that the adsorption is spontaneous at all the temperatures. The positive value of ΔH^0 confirms the endothermic nature of adsorption, while the positive value for ΔS^0 suggests an increased randomness at the solution/solid interface during MB adsorption on the activated carbon.

Adsorption capacity

Table 14 shows a comparison of monolayer adsorption of MB onto activated carbon from different precursors.

Table 14 | Comparison of maximum monolayer adsorption of MB onto activated carbon from different precursors

Precursor	Agent	Adsorption capacity (mg/g)	Reference
Cotton stalk	$ZnCl_2$	193.50	Deng *et al.* (2009)
Water hyacinth		2.70	Kanawade & Gaikwad (2011)
Lupinus albus	$ZnCl_2$	109.89	Bağcı & Ceyhan (2015)
Jatropha curcas fruit	KOH/ NaCl	87.70	Okeola *et al.* (2012)
Euphorbia rigida	H_2SO_4	114.50	Gercel *et al.* (2007)
Pistachio shells	H_3PO_4	129	Attia *et al.* (2003)
Tobacco stems	$ZnCl_2$	123.45	Present study

The referred studies show that activated carbon prepared with zinc chloride activation has generally high adsorption capacity for MB. This could, however, be a factor of the precursor material as well as the activation procedure. Studies could as well be conducted using different activation agents on the same precursor material.

CONCLUSION

This study revealed that tobacco stalks are ideal precursor material for activated carbon preparation due to their highly carbonaceous nature. The microwave method used in this experiment proved to be much faster, requiring only 6 minutes to carbonize the raw material, compared with the muffle furnace method, which might have required many hours. The optimum conditions of activated carbon preparation obtained from this study are a microwave power of 208 W, radiation time of 6 minutes and impregnation time of 24 hours with 30% $ZnCl_2$. These conditions gave a yield of 49.43%. Similar yields were also obtained by other researchers who have used different precursor materials before. The point of zero charge of 5.81 indicated that the activated carbon has net electrical neutrality in acidic conditions, a factor which favours adsorption of cationic species within this pH range. The activated carbon product also had a high level of carbon content with low mineral content, making it ideal for application in water treatment. The functional group analysis for the activated carbon shows the presence of O-H, -C-C-, -C-O- and -C-H- bands in alkynes, an indication of multiple carbon–carbon bond formation. The BET surface area of the activated carbon was found to be 684.68 m^2/g with a pore volume of 00.45 cm^3/g. The adsorption of MB was shown to be affected by adsorption parameters including adsorption time, pH of solution, initial analyte concentration and activated carbon dosage. The adsorption mechanism obeys the pseudo second order kinetic model with the intra-particle diffusion data suggesting that adsorption is in two phases, first with adsorption on the surface adsorbent site and then diffusion from the film surface into the micropores. Experimental data for the MB adsorption also fit well into the Langmuir isotherm model with an adsorption capacity of 123.46 mg/g. The results of this study indicated that tobacco stalks can be turned into a useful product for water purification. This would specifically help to reduce the environmental cost of waste disposal.

REFERENCES

Amuda, O. S., Olayiwola, A. O., Alade, A. O., Farombi, A. G. & Adebisi, S. A. 2014 Adsorption of methylene blue from aqueous solution using steam-activated carbon produced from *Lantana camara* stem. *Journal of Environmental Protection* **5**, 1352.

ASTM 2006 *Standard Test Method for Determination of Iodine Number of Activated Carbon1*.

Attia, A., Girgis, B. S. & Khedr, S. A. 2003 Capacity of activated carbon derived from pistachio shells by H_3PO_4 in the removal of dye and phenolics. *Journal of Chemical Technology and Biotechnology* **78**, 611–619.

Bağcı, S. & Ceyhan, A. A. 2015 Adsorption of methylene blue onto activated carbon prepared from *Lupinus albus*. *Chemical Industry and Chemical Engineering Quarterly* **22** (2), 155–165.

Bhatnagar, A. & Minocha, A. 2006 Conventional and non-conventional adsorbents for removal of pollutants from water-a review. *Indian Journal of Chemical Technology* **13**, 203–217.

Deng, H., Yang, L., Tao, G. & Dai, J. 2009 Preparation and characterization of activated carbon from cotton stalk by microwave assisted chemical activation-application in methylene blue adsorption from aqueous solution. *Journal of Hazardous Materials* **166**, 1514–1521.

Gercel, O., Ozcan, A., Ozcan, A. & Gercel, H. F. 2007 Preparation of activated carbon from a renewable bio-plant of *Euphorbia rigida* by H_2SO_4 activation and its adsorption behaviour in aqueous solutions. *Applied Surface Science* **253**, 4843–4852.

Ghosh, R. K. & Reddy, D. D. 2013 Tobacco stem ash as an adsorbent for removal of methylene blue from aqueous solution: equilibrium, kinetics, and mechanism of adsorption. *Water, Air, & Soil Pollution* **224**, 1–12.

Kanawade, S. M. & Gaikwad, R. 2011 Removal of methylene blue from effluent by using activated carbon and water hyacinth as adsorbent. *International Journal of Chemical Engineering and Applications* **2**, 317.

Li, W., Zhang, L.-B., Peng, J.-H., Li, N. & Zhu, X.-Y. 2008 Preparation of high surface area activated carbons from tobacco stems with K_2CO_3 activation using microwave radiation. *Industrial Crops and Products* **27**, 341–347.

Lori, J. A., Lawal, A. O. & Ekanem, E. J. 2008 Adsorption characteristics of activated carbons from pyrolysis of bagasse, sorghum and millet straw in orthophosphoric acid. *Journal of Environmental Science and Technology* **1**, 124–134.

Makeswari, M. & Santhi, T. 2012 Optimization of preparation of activated carbon from *Ricinus communis* leaves by microwave-assisted zinc chloride chemical activation: competitive adsorption of Ni^{2+}. *Journal of Chemistry* **2013**, 1–12.

Mohan, D., Singh, K., Singh, G. & Kumar, K. 2002 Removal of dyes from wastewater using fly ash a low-cost adsorbent. *Industrial & Engineering Chemistry Research* **41**, 3688–3695.

Muthuraman, G., Tow, T., Peng, L. & Ismail, N. 2008 Recovery and reuse of methylene blue from industrial wastewater using benzoic acid as a carrier. In: *International Conference on*

Environmental Research and Technology (ICERT), University Sains Malaysia, Malaysia, pp. 278–282.

Namasivayam, C. & Sangeetha, D. 2005 Removal and recovery of nitrate from water by $ZnCl_2$ activated carbon from coconut coir pith, an agricultural solid waste. *Indian Journal of Chemical Technology* **12**, 513.

Oguz, E. & Keskinler, B. 2007 Comparison among O_3, PAC adsorption, O_3/HCO_3, O_3/H_2O_2 and O_3/PAC processes for the removal of Bomaplex Red CR-L dye from aqueous solution. *Dyes Pigments* **74**, 329–334.

Okeola, O., Odebunmi, E. & Ameen, O. 2012 Comparison of sorption capacity and surface area of activated carbon prepared from *Jatropha curcas* fruit pericarp and seed coat. *Bulletin of the Chemical Society of Ethiopia* **26** (2), 171–180.

Qi, B. & Aldrich, C. 2008 Biosorption of heavy metals from aqueous solutions with tobacco dust. *Bioresource Technology* **99**, 5595–5601.

Ren, L., Zhang, J., Li, Y. & Zhang, C. 2011 Preparation and valuation of cattail fibre-based activated carbon for 2,4-dichlorophenol and 2,4,6-trichlorophenol removal. *Chemical Engineering Journal* **168**, 553–561.

Said, A., Hakim, M. S. & Rohyami, Y. 2014 The effect of contact time and pH on methylene blue removal by volcanic ash. In: *International Conference on Chemical, Biological and Environmental Sciences (ICCBES'14), Malaysia*. Kuala Lumpur, Malaysia, pp. 11–13.

Tahiruddin, N. S. M. & Ab Rahman, S. Z. 2013 Adsorption of lead in aqueous solution by a mixture of activated charcoal and peanut shell. *World Journal of Science and Technology Research* **1**, 102–109.

Tamilselvi, S. & Asaithambi, M. 2015 Microwave assisted synthesis of activated carbon fibres from silk cotton. *International Journal of ChemTech Research* **7**, 375–381.

Wang, S., Boyjoo, Y., Choueib, A. & Zhu, Z. 2005 Removal of dyes from aqueous solution using fly ash and red mud. *Water Research* **39**, 129–138.

Zhong, Z.-Y., Yang, Q., Li, X.-M., Luo, K., Liu, Y. & Zeng, G.-M. 2012 Preparation of peanut hull-based activated carbon by microwave-induced phosphoric acid activation and its application in Remazol Brilliant Blue R adsorption. *Industrial Crops and Products* **37**, 178–185.

First received 13 September 2016; accepted in revised form 9 January 2017. Available online 1 March 2017